**Protein Engineering, Design & Selection** vol. 25 no. 10 pp. 581–589, 2012
Published online August 30, 2012 doi:10.1093/protein/gzs055

# Disulfide linkage engineering for improving biophysical properties of human $V_H$ domains[6]

**Dae Young Kim[1], Hiba Kandalaft[1], Wen Ding[1], Shannon Ryan[1], Henk van Faassen[1], Tomoko Hirama[1,4], Simon J. Foote[1], Roger MacKenzie[1,2] and Jamshid Tanha[1,2,3,5]**

[1]Human Health Therapeutics, National Research Council Canada, Ottawa, ON, Canada K1A 0R6, [2]School of Environmental Sciences, Ontario Agricultural College, University of Guelph, Guelph, ON, Canada N1G 2W1, [3]Department of Biochemistry, Microbiology and Immunology, University of Ottawa, Ottawa, ON, Canada K1N 6N5 and [4]Present address: 50-2704 Miyamchi 1-chome, Fuchu, Tokyo, Japan, 183-0023

[5]To whom correspondence should be addressed.
E-mail: jamshid.tanha@nrc-cnrc.gc.ca

**Received March 23, 2012; revised August 1, 2012; accepted August 8, 2012**

**Edited by Laurent Jespers**

**To enhance their therapeutic potential, human antibody heavy chain variable domains ($V_H$s) would benefit from increased thermostability. The highly conserved disulfide linkage that connects Cys23 and Cys104 residues in the core of $V_H$ domains is crucial to their stability and function. It has previously been shown that the introduction of a second disulfide linkage can increase the thermostability of camelid heavy-chain antibody variable domains ($V_H$Hs). Using four model domains we demonstrate that this strategy is also applicable to human $V_H$ domains. The introduced disulfide linkage, formed between Cys54 and Cys78 residues, increased the thermostability of $V_H$s by 14–18°C. In addition, using a novel hexa-histidine capture technology, circular dichroism, turbidity, size exclusion chromatography and multiangle light scattering measurements, we demonstrate reduced $V_H$ aggregation in domains with the Cys54–Cys78 disulfide linkage. However, we also found that the engineered disulfide linkage caused conformational changes, as indicated by reduced binding of the $V_H$s to protein A. This indicates that it may be prudent to use the synthetic $V_H$ libraries harboring the engineered disulfide linkage before screening for affinity reagents. Such strategies may increase the number of thermostable binders.**

*Keywords*: aggregation/antibody variable domains/disulfide linkage engineering/synthetic $V_H$ libraries/thermostability

## Introduction

Protein stability is a key to the performance of protein therapeutics. Unstable proteins often aggregate or partially unfold. This leads to undesirable consequences *in vivo* such as increased susceptibility to degradation, decreased serum half-life, immunogenic reactions or non-specific antigenic recognition (Mitraki and King, 1992; Hurle *et al.*, 1994; Wetzel, 1994; Wörn and Plückthun, 2001; Horwich, 2002; Frokjaer and Otzen, 2005). The end result is reduced therapeutic efficacy.

Human $V_H$ domains form an important class of biologics. Aggregation was recognized as a major drawback of $V_H$s, as early as 1989 (Ward *et al.*, 1989); however, significant advances since then have made the generation of non-aggregating $V_H$s a routine exercise. For example, selection approaches have been developed that allow for efficient screening of synthetic human $V_H$ libraries for $V_H$ binders that are non-aggregating and have high thermodynamic stability (Jespers *et al.*, 2004; To *et al.*, 2005; Famm *et al.*, 2008; Arbabi-Ghahroudi *et al.*, 2009a,b, 2010). Site-specific mutagenesis approaches for improving the non-aggregation character of $V_H$ domains have also been developed (Arbabi-Ghahroudi *et al.*, 2009a, 2010). Novel complementary and/or generic mutagenesis approaches that render $V_H$s non-aggregating are desirable; more desirable are the approaches that also stabilize $V_H$ domains in a multifaceted manner.

The sole disulfide bond connecting β-strands B and F of $V_H$ domains is highly conserved (Amzel and Poljak, 1979; Williams and Barclay, 1988). Linking Cys23 and Cys104 residues in the core of $V_H$s, its loss leads to a dramatic decrease in the thermodynamic stability, misfolding and non-functionality (Goto and Hamaguchi, 1979; Proba *et al.*, 1998; Ciaccio and Laurence, 2009). It follows that adding extra disulfide linkage(s) at optimal positions should increase $V_H$ stability as it has been shown in several instances, including Ig domains (Wetzel *et al.*, 1988; Matsumura *et al.*, 1989; Betz, 1993; Young *et al.*, 1995; Davies and Riechmann, 1996; Mansfeld *et al.*, 1997; Hagihara *et al.*, 2007; Chan *et al.*, 2008; Saerens *et al.*, 2008; Gong *et al.*, 2009; Hussack *et al.*, 2011; Govaert *et al.*, 2012; Wozniak-Knopp *et al.*, 2012). Disulfide linkages stabilize proteins by reducing their conformational entropy through limiting the number of possible conformers that lead to unfolded states (Fersht, 1997; Mason *et al.*, 2002).

Recently, it was shown that the engineering of a second Cys54–Cys78 disulfide linkage, which bridges β-strands C′ and D, into camelid heavy-chain antibody variable domains, $V_H$Hs, increased their thermal and chemical stabilities (Hagihara *et al.*, 2007; Chan *et al.*, 2008; Saerens *et al.*, 2008; Hussack *et al.*, 2011). Here, we show that the application of the same disulfide linkage engineering approach to $V_H$s leads to increases in the thermostability of $V_H$s as well, with additional improvements in $V_H$ non-aggregation.

## Materials and methods

### *Cloning, expression and mass spectrometry analysis*

Mutant $V_H$s, huVHAm302S, huVHAm427S, huVHAm431S and huVHPC235S with Cys substitutions at positions 54 and

[6]This is National Research Council Canada Publication Number 50020.

78 were created from their corresponding wild-type $V_H$s, huVHAm302, huVHAm427, huVHAm431 and huVHPC235, respectively, by the splice overlap extension-polymerase chain reaction approach (Ho *et al.*, 1989; Arbabi-Ghahroudi *et al.*, 2010). $V_H$s were cloned, expressed and purified by immobilized metal ion affinity chromatography (IMAC) as described (Arbabi-Ghahroudi *et al.*, 2009a). The purity of $V_H$s was subsequently assessed by sodium dodecyl sulfate-polyacrylamide gel electrophoresis (SDS-PAGE).

To verify the presence/absence of the Cys54–Cys78 disulfide linkage, $V_H$s were digested with trypsin and chymotrypsin and the generated peptides were subjected to mass spectrometry (MS) analysis as described in the legend of Supplementary Fig. S2.

### *Melting temperature and fraction refolded determinations*

Circular dichroism (CD) spectra and melting temperature ($T_m$) measurements were obtained as described by Kim *et al.* (2012) using a Jasco J-815 spectropolarimeter equipped with a Peltier thermoelectric-type temperature control system (Jasco, Easton, MD, USA). The determination of the reversibility of the temperature-induced denaturation and the estimation of the fraction of refolded protein recovered following thermal denaturation were carried out according to previously described protocols (Barthelemy *et al.*, 2008). Purified monomeric $V_H$s (50 μg/ml in 0.1 M sodium phosphate buffer, pH 7.4) obtained by size exclusion chromatography (see below and Supplementary Fig. S3) were used for CD, $T_m$ and fraction refolded measurements, with CD parameters set as follows: bandwidth = 1 nm; temperature range = 30–96°C; temperature ramp = 1°C/min; data collection = every 1°C; DIT = 4 s; and accumulations = 1. Ellipticity changes at 210 nm (huVHAm431 and huVHAm431S), 205 nm (huVHAm427, huVHAm427S, huVHAm302 and huVHAm302S), 220 nm (huVHPC235) and 200 nm (huVHPC235S) were used for the construction of thermal unfolding curves and subsequent calculation of $T_m$s and fraction refolded values. With the huVHAm427S and huVHAm431S unfolding transition curves, which had no clear lower plateau, ellipticity values at 96°C were taken as the lower plateaus for constructing melting curves and subsequent determination of $T_m$s. Therefore, the $T_m$s for both huVHAm427S and huVHAm431S are estimated minimum $T_m$s.

### *Size exclusion chromatography and multiangle light scattering analyses*

Two hundred microlitres of $V_H$s (0.25 mg/ml) dialyzed in phosphate-buffered saline (137 mM NaCl, 2.7 mM KCl, 4.3 mM $Na_2HPO_4$, 1.47 mM $KH_2PO_4$, pH 7.4) plus 0.5 mM ethylenediaminetetraacetic acid (PBS/EDTA)—and free of any insoluble aggregates as determined by turbidity measurements at 360 nm—were applied at a flow rate of 0.5 ml/min to a Superdex™ 75 10/300 GL column (GE Healthcare, Baie d'Urfé, QC, Canada) equilibrated with 4-(2-hydroxyethyl)-1-piperazineethanesulfonic acid (HEPES) buffered saline containing EDTA and polysorbate 20 buffer (10 mM HEPES, 150 mM NaCl, 3 mM EDTA and 0.005% P20 surfactant, pH 7.4). Size exclusion experiments were carried out at room temperature and chromatograms were obtained. For each chromatogram, background absorbance was subtracted and all peaks were normalized with respect to the monomeric peak, which was arbitrarily set at 100%. Peaks to the left of monomeric peaks were considered to be aggregate peaks. Peak areas, $A$, were determined by integration using ÄKTA FPLC (GE Healthcare) operating software UNICORN (version 5.1 for Windows). %Aggregate was determined by the formula: $\%\text{Aggregate} = ((A_{\text{aggregate}})/(A_{\text{aggregate}} + A_{\text{monomer}}))$, where $A_{\text{aggregate}}$ is the area of aggregate peaks and $A_{\text{monomer}}$ is the area of the monomer peak. %Aggregate was not determined for huVHAm427 as its monomeric peak was not considered authentic due to peak tailing. %Aggregate values are recorded in Table II. %Recovery was determined as described in the legend of Supplementary Fig. S4 and recorded in Table II.

Clear $V_H$ samples (0.55–0.8 mg/ml) were subjected to size exclusion chromatography as described above with PBS as the equilibration buffer, and the molecular weights of the monomeric species were confirmed by multiangle light scattering using a tri-angle light scattering detector (miniDawn Treos; Wyatt Technology, Santa Barbara, CA, USA). Experiments were performed in duplicates.

### *Turbidity analysis*

In brief, to measure turbidity, $V_H$s were dialyzed in PBS/EDTA, centrifuged in a microfuge at 13 000 rpm for 1 min, and their concentrations were adjusted to 100 μg/ml. Sample absorbance ($A_{360nm}$) was taken at room temperature in a spectrophotometer using a 100-QS, 1 mm path length Absorbance Cell (Hellma Analytics, Müllheim, Germany). The samples were then heated to 80°C for 20 min, cooled at room temperature for 20 min, centrifuged for a few seconds to collect condensation, pipetted up and down a few times and their $A_{360nm}$ was measured once again. All treated and untreated samples, including a non-aggregating llama $V_HH$ control (A4.2; Hussack *et al.*, 2011) had the same $A_{360nm}$ as the background sample (PBS/EDTA) indicating the absence of turbidity. Turbidity measurements were performed in duplicates.

### *Surface plasmon resonance analysis*

Surface plasmon resonance (SPR) analysis of $V_H$ binding to a $Ni^{2+}$-NTA sensorchip was carried out. A control llama $V_HH$ monomer (A4.2) and a control $V_H$ homodimer (Baral *et al.*, 2012) were also included in the analysis. All $V_H$/$V_HH$ domains had $His_6$ tags at their C-termini. The $V_H$ homodimer is formed by the non-covalent association of two $V_H$ monomer units and as a result has two C-terminal $His_6$ tags. $V_H$ domains huVHAm302S, huVHAm427S and huVHAm431S were not included in the analysis as, unlike the control domains, they had $His_5$ tags. SPR experiments were carried out with protein fractions corresponding to the dimeric peak in the case of the $V_H$ dimer control and monomeric peaks for the remaining $V_H$/$V_HH$ domains. Resonance units (RUs) from duplicate data sets were averaged and then normalized to obtain %RU. The binding of $V_H$s/$V_HH$ to an activated NTA sensorchip was determined by SPR using a BIACORE 3000 (GE Healthcare). In each cycle, 0.5 mM $NiCl_2$ was injected at 5 μl/min for 2 min, followed by an injection of 50 nM $V_H$/$V_HH$ in running buffer (10 mM HEPES, 150 mM NaCl, 0.005% P20 surfactant, 50 μM EDTA, pH 7.4) at a flow rate of 5 μl/min with an injection time of 5 min and a dissociation time of 10 min. Sensorgrams were run in duplicates. The NTA chip was regenerated with 350 mM EDTA in 10 mM HEPES, 150 mM NaCl at pH 8.4 for 3 min before the next cycle. Analyses were carried out at 25°C in running buffer. Dissociation rate

constants ($k_{off}$s) were obtained over 60 s time periods between 315–375 s and 780–840 s. Data were analyzed with BIAevaluation 4.1 software (GE Healthcare). SPR analyses of $V_H$ binding to protein A were carried out as described in the legend of Supplementary Fig. S6.

## Results

### *Mutant $V_H$s with Cys54 and Cys78 substitutions are readily expressed in soluble forms*

We chose four human $V_H$s for this study: huVHAm302, huVHAm427, huVHAm431 and huVHPC235, all with protein A binding activity (Fig. 1a). huVHAm302, huVHAm427 and huVHAm431 additionally bind to α-amylase (Arbabi-Ghahroudi *et al.*, 2009b), whereas the antigen specificity of huVHPC235 is not known. By size exclusion chromatography, the first three $V_H$s were aggregation prone, whereas huVHPC235 appeared to be non-aggregating. Employing the splice overlap extension-polymerase chain reaction approach, we created the mutant versions by introducing Cys pairs at positions 54 and 78 (Fig. 1). The mutants, designated as huVHAm302S, huVHAm427S, huVHAm431S and huVHPC235S, were cloned, expressed and purified by IMAC. Results showed that the mutant $V_H$s had expression yields comparable with their wild-type counterparts (Supplementary Fig. S1a), indicating that the engineered disulfide linkage had no adverse effect on the expression of $V_H$s. We observed that the three aggregating wild-type $V_H$s eluted significantly later than their corresponding mutant versions, indicating tighter binding of the wild-type $V_H$s to the purification column. This could be due to the fact that the aggregating wild-type $V_H$s may additionally interact with the column materials through non-specific interactions and/or coordinate tighter to the column nickel due to the presence of multiple His-tags on aggregates. We also noticed that the mutant $V_H$s migrated slower than their wild-type counterparts on non-reducing SDS-PAGE gels, with migration differences disappearing under reducing conditions (Supplementary Fig. S1b). Such SDS-PAGE mobility patterns have been seen in the case of $V_H$Hs as well, and it was suggested that this indicates Cys54–Cys78 disulfide linkage formation in extra Cys mutants (Hussack *et al.*, 2011).

### *Cys54 and Cys78 residues form a disulfide linkage in mutant $V_H$s*

Next, we aimed to verify by MS if the engineered Cys54 and Cys78 in mutant $V_H$s formed a disulfide linkage. Wild type and mutant $V_H$s were digested with trypsin or a trypsin–chymotrypsin combination and the generated proteolytic peptides were subjected to $MS^2$ analysis (Supplementary Fig. S2) (Wu *et al.*, 2009; Hussack *et al.*, 2011; Kim *et al.*, 2012). huVHAm302, huVHAm302S and huVHPC235S were readily digested with trypsin (Supplementary Fig. S2a). From our MS results with trypsinized huVHAm302S and huVHPC235S, we successfully identified disulfide linked peptides (Supplementary Fig. S2; Table I). The identification coverage of each protein from the analysis of their tryptic digests using nano-RPLC-$MS^2$ with data-dependent analysis (DDA) was more than 30%, where the disulfide-linked peptide ions appeared prominent in the survey scan of the

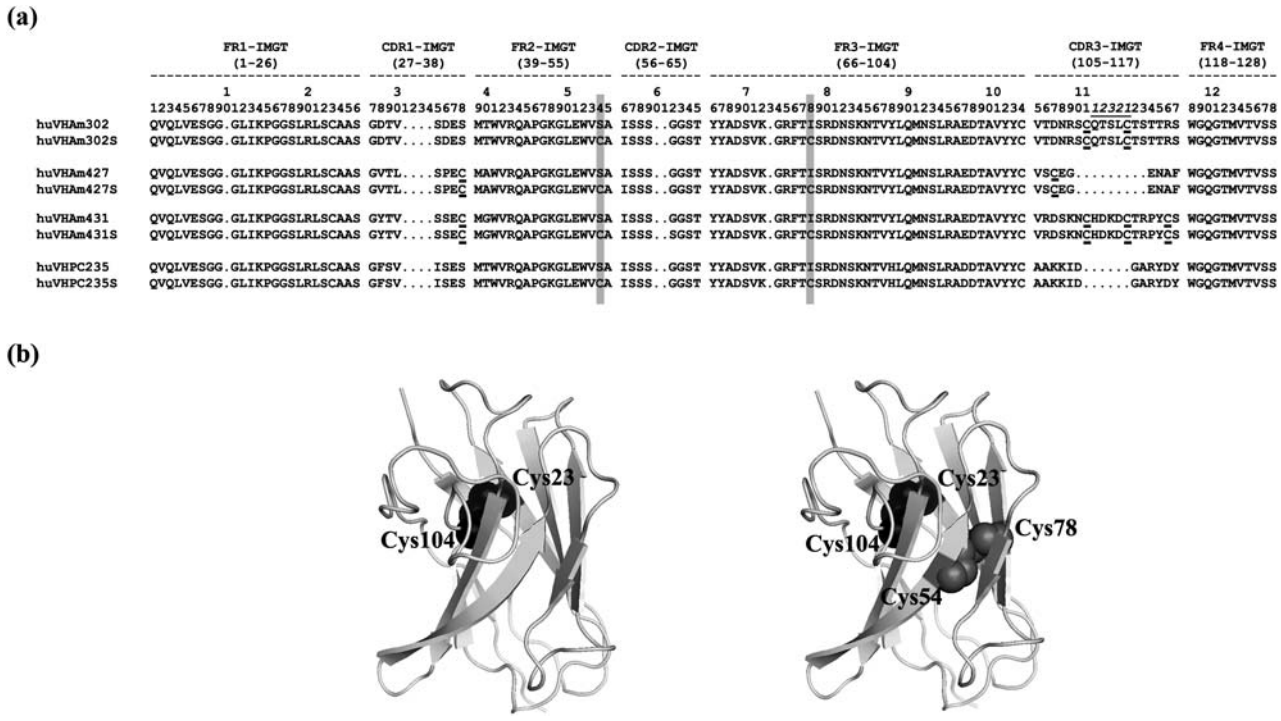


**Fig. 1.** Structures of $V_H$s. (**a**) Amino acid sequence of the $V_H$s used in this study. Numbering and CDR designations are according to the ImMunoGeneTics (IMGT) numbering system and definitions (http://www.imgt.org). The underlined numbers 1, 2, 3, 2, 1 in the CDR3 represent amino acid positions 111.1, 111.2, 112.3, 112.2 and 112.1, respectively. Positions 54 and 78, mutated to Cys in mutant $V_H$s, are highlighted in gray. Other non-canonical Cys residues are underlined. FR, framework region. (**b**) Representative homology structure model of wild type (left) and mutant (right) huVHAm302. The canonical (Cys23–Cys104) and engineered (Cys54–Cys78) disulfide linkages are shown in black and gray spheres, respectively. The protein structures were obtained using the Geno3D automatic modeling tool (http://pbil.ibcp.fr/htm/index.php). The figures were drawn using PyMOL (http://www.pymol.org) and Disulfide by Design (version 1.20) freeware (Dombkowski, 2003).

**Table I.** Disulfide linkage determination of $V_H$s by MS

| $V_H$ | Tryptic peptides[a] | | $MW_{for}$ (Da) | $MW_{exp}$ (Da) | $\Delta MW$[c] (Da) |
|---|---|---|---|---|---|
| huVHAm302 | S**C**QTSL**C**TSTTR | | 1284.54 | 1284.55 | −0.01 |
| | LS**C**AASGDTVSDESMTWVR | AEDTAVYY**C**VTDNR | 3630.55 | 3630.52 | 0.03 |
| huVHAm302S | S**C**QTSL**C**TSTTR | | 1284.54 | 1284.56 | −0.02 |
| | GLEWV**C**AISSSGGSTYYADSVK | FT**C**SR | 2889.28[b] | 2889.30[b] | −0.02[b] |
| | LS**C**AASGDTVSDESMTWVR | AEDTAVYY**C**VTDNR | 3630.55 | 3630.52 | 0.03 |
| huVHAm427 | LS**C**AASGVTL | **C**VS | 1225.57 | 1225.64 | −0.07 |
| huVHAm427S | LS**C**AASGVTL | **C**VS | 1225.57 | 1225.64 | −0.07 |
| | V**C**AISSSGGSTY | FT**C**SR | 1740.74[b] | 1740.81[b] | −0.07[b] |
| | V**C**A | FT**C**SR | 901.38[b] | 901.44[b] | −0.06[b] |
| huVHAm431 | LS**C**AASGY | **C**VR | 1144.50 | 1144.51 | −0.01 |
| | TVSSE**C**M | **C**SW | 1147.40 | 1147.47 | −0.07 |
| huVHAm431S | LS**C**AASGY | **C**VR | 1144.50 | 1144.46 | 0.04 |
| | V**C**AISSSSGSTY | T**C**SR | 1623.68[b] | 1623.62[b] | 0.06[b] |
| | TVSSE**C**M | **C**SW | 1147.40 | 1147.45 | −0.05 |
| huVHPC235S[d] | GLEWV**C**AISSSGGSTYYADSVK | FT**C**SR | 2889.28[b] | 2889.30[b] | −0.02[b] |
| | LS**C**AASGFSVISESMTWVR | AEDTAVYY**C**AAK | 3331.51 | 3331.47 | 0.04 |

[a]Major tryptic or tryptic/chymotryptic peptides containing disulfide linkages are shown, with connecting cysteine residues underlined and boldfaced (see Supplementary Fig. S2 for experimental details). Non-specific or miscleavage occurred during the trypsin/chymotrypsin digestion of huVHAm427 and huVHAm431 and their mutant versions. Spaces within peptide doublets denote sequence discontinuity.
[b]The very close match between $MW_{for}$ (formula molecular weight) and $MW_{exp}$ (experimental molecular weight) indicates the presence of the Cys54–Cys78 disulfide linkage.
[c]$\triangle MW = MW_{for} - MW_{exp}$.
[d]The wild-type huVHPC235 contains only one pair of Cys, the conserved Cys23 and Cys104 residues which always form a disulfide linkage.

DDA experiment. The expected disulfide-linked peptide sequences corresponding to each $V_H$ were all confirmed by manual *de novo* sequencing. In the case of huVHAm302S, a prominent ion at m/z 964.04 (3+) was sequenced as GLEWVCAISSSGGSTYYADSVK (P1) disulfide-linked to FTCSR (P2) as shown (Supplementary Fig. S2b), indicating the existence of a Cys54–Cys78 disulfide linkage. A complete disulfide-linked y fragment ion series was observed from P1 with P2 linked via a disulfide linkage, which remained intact under collision-induced dissociation (Supplementary Fig. S2; Table I). The formation of the Cys54–Cys78 disulfide linkage was also verified for huVHPC235S (Table I; $MS^2$ spectrum not shown). Disulfide linkages between Cys23 and Cys104, and Cys111 and Cys112.1 were also identified by MS for both huVHAm302 and huVHAm302S (Table I). huVHAm427, huVHAm427S, huVHAm431 and huVHAm431S were highly protease resistant, and therefore, had to be treated with a higher amount of trypsin (huVHAm427 and huVHAm427S) or a higher amount of trypsin plus chymotrypsin (huVHAm431 and huVHAm431S) for the MS analyses. Following protease digestions, the existence of disulfide linkages was verified by *de novo* sequencing with the assistance of the DBond program. DBond v2.07 was used to generate the potential disulfide-linked peptide ions corresponding to non-specifically cleaved or miscleaved peptides (Choi *et al.*, 2010). The resulting output was parsed for disulfide-linked peptides with match-quality scores >15 and the corresponding raw data were analyzed for matching ions to guide subsequent manual validation and targeted $MS^2$ experiments to obtain $MS^2$ spectra for *de novo* sequencing. The results showed the existence of the Cys54–Cys78 disulfide linkage in huVHAm427S and huVHAm431S (Table I; $MS^2$ spectra not shown). In addition, the conserved Cys23–Cys104 disulfide linkage was also verified by MS in all four wild type and mutant $V_H$s. Both huVHAm427/huVHAm427S and huVHAm431/huVHAm431S pairs also have a pair of Cys at complementarity-determining region 1 (CDR1) position 38 and CDR3 positions 107 or 116, respectively (Fig. 1a). However, only in the case of the huVHAm431/huVHAm431S pair, were we able to show the existence of an inter-CDR1–CDR3 disulfide linkage (Cys38–Cys116). In addition, we could not determine whether Cys111 and Cys112.1 in huVHAm431 and huVHAm431S $V_H$s (Fig. 1a) formed disulfide linkages. The slower non-reducing SDS-PAGE mobilities compared with corresponding wild-type $V_H$s is consistent with the presence of the extra Cys54–Cys78 disulfide linkage in mutant $V_H$s (see above).

### *Mutant $V_H$s are far more thermostable than the wild-type counterparts*

To assess the effect of the engineered disulfide linkage on the thermostability of $V_H$s, we determined the thermal unfolding midpoint temperatures ($T_m$s) of the $V_H$s by CD spectrometry. All $V_H$s exhibited the two-state sigmoidal melting curves typical of single-domain antibodies. We found that mutant $V_H$s had significantly higher $T_m$s compared with their corresponding wild-type counterparts (Fig. 2a and b; Supplementary Fig. S3; Table II) (paired *t*-test, two-tailed, $P = 0.0002$). The wild-type $V_H$s had $T_m$s of 53.8–73.0°C which increased to 71.4–89.2°C for mutant $V_H$s. This corresponds to $T_m$ increases ($\Delta T_m$s) of 13.9–17.6°C. By comparing disulfide linkage patterns of mutant vs. wild-type $V_H$s (Table I), it is clear that the $T_m$ increases are due to the presence of the extra Cys54–Cys78 disulfide linkage. Unlike huVHAm302S and huVHAPC235S, huVHAm427S and huVHAm431S had unusually high $T_m$s, 89.2 and 87.5°C, respectively, most likely due to the presence of a second non-canonical, inter-CDR1–CDR3 disulfide linkage (Fig. 1a; Tables I and II), in addition to the conserved Cys23–Cys104 disulfide linkage common to all $V_H$s. Previous studies showed that inter-CDR1–CDR3 disulfide linkages stabilized (e.g. thermostabilized) human $V_H$s and camelid $V_HH$s (Davies and Riechmann, 1996; Arbabi-Ghahroudi *et al.*, 2009b; Govaert *et al.*, 2012). The high $T_m$s of huVHAm427S and huVHAm431S explain why these two

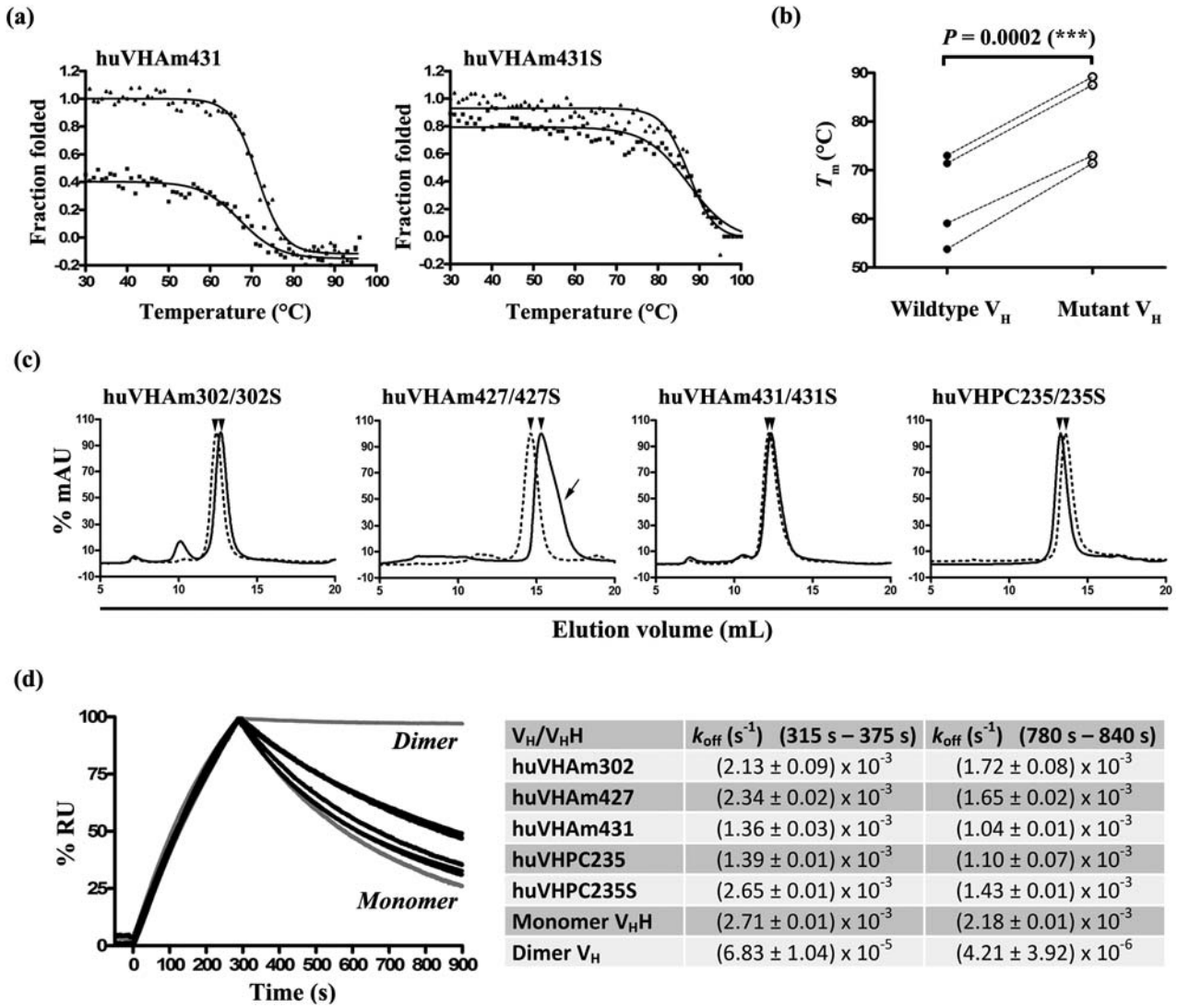


| $V_H$/$V_H$H | $k_{off}$ ($s^{-1}$) (315 s – 375 s) | $k_{off}$ ($s^{-1}$) (780 s – 840 s) |
|---|---|---|
| huVHAm302 | $(2.13 \pm 0.09) \times 10^{-3}$ | $(1.72 \pm 0.08) \times 10^{-3}$ |
| huVHAm427 | $(2.34 \pm 0.02) \times 10^{-3}$ | $(1.65 \pm 0.02) \times 10^{-3}$ |
| huVHAm431 | $(1.36 \pm 0.03) \times 10^{-3}$ | $(1.04 \pm 0.01) \times 10^{-3}$ |
| huVHPC235 | $(1.39 \pm 0.01) \times 10^{-3}$ | $(1.10 \pm 0.07) \times 10^{-3}$ |
| huVHPC235S | $(2.65 \pm 0.01) \times 10^{-3}$ | $(1.43 \pm 0.01) \times 10^{-3}$ |
| Monomer $V_H$H | $(2.71 \pm 0.01) \times 10^{-3}$ | $(2.18 \pm 0.01) \times 10^{-3}$ |
| Dimer $V_H$ | $(6.83 \pm 1.04) \times 10^{-5}$ | $(4.21 \pm 3.92) \times 10^{-6}$ |

**Fig. 2.** Thermostability and aggregation state of $V_H$s. (**a**) Representative example showing the thermal unfolding curves of huVHAm431 and huVHAm431S (see Supplementary Fig. S3 for unfolding curves for all $V_H$s and experimental details). The upper and lower thermal unfolding curves correspond to ellipticity measurements obtained upon first and second heating, respectively. $T_m$s (the midpoint temperatures of unfolding curves) and fraction refolded values are recorded in Table II. (**b**) Graph comparing the $T_m$s of wild type and corresponding mutant $V_H$s. (**c**) Aggregation state of $V_H$s determined by analytical Superdex$^{TM}$ 75 size exclusion chromatography. The elution volumes for monomeric peaks (marked by arrowheads) were 12.7 ml (huVHAm302), 12.4 ml (huVHAm302S), 15.3 ml (huVHAm427), 14.6 ml (huVHAm427S), 12.3 ml (huVHAm431), 12.2 ml (huVHAm431S), 13.3 ml (huVHPC235) and 13.6 ml (huVHPC235S). Peaks to the left of monomeric peaks were considered to be aggregate peaks. huVHAm427 monomeric peak shows tailing (marked by an arrow). (**d**) SPR analysis of $V_H$ binding to a $Ni^{2+}$-NTA sensorchip. A control llama $V_H$H monomer (A4.2; Hussack *et al.*, 2011) and a control $V_H$ dimer (Baral *et al.*, 2012) were also included in the analysis.

**Table II.** Biophysical properties of $V_H$s

| $V_H$ | $T_m$ (°C)[a] | $\Delta T_m$ (°C)[a] | Fraction refolded[a,d] | $K_D$ (μM) | %Aggregate[a] | %Recovery[a,e] | $MW_{for}$ (kDa) | $MW_{exp}$ (kDa)[a] |
|---|---|---|---|---|---|---|---|---|
| huVHAm302 | 53.8 ± 0.1 | 17.6 ± 0.22 | 0.60 ± 0.12 | 3 | 13.9 ± 0.02 | 69 ± 0.6 | 15.56 | 18.33 ± 0.04 |
| huVHAm302S | 71.4 ± 0.2 | | 0.46 ± 0.07 | 10 | 4.1 ± 0.15 | 76 ± 0.1 | 15.43 | 16.73 ± 0.75 |
| huVHAm427 | 73.0 ± 0.3 | 16.2 ± 2.6[c] | 0.84 ± 0.04 | 1.6 | 3.8 ± 2.9 | NA | 14.52 | 16.35[f] |
| huVHAm427S | 89.2 ± 2.6[b] | | 0.75 ± 0.11 | 4 | 6.6 ± 0.76 | 78 ± 0.3 | 14.39 | 15.27 ± 0.53 |
| huVHAm431 | 71.4 ± 0.4 | 16.1 ± 0.45[c] | 0.45 ± 0.02 | 4 | 5.5 ± 0.08 | 82 ± 0.5 | 15.43 | 17.95 ± 0.62 |
| huVHAm431S | 87.5 ± 0.2[b] | | 0.89 ± 0.07 | 8 | 4.3 ± 0.14 | 100 ± 1.9 | 15.62 | 17.05 ± 0.30 |
| huVHPC235 | 59.1 ± 0.2 | 13.9 ± 0.20 | 0.58 ± 0.05 | 0.3 | 0 ± 0.02 | 70 ± 3.7 | 14.95 | 15.03 ± 0.09 |
| huVHPC235S | 73.0 ± 0.0 | | 0.75 ± 0.08 | 3 | 0.6 ± 0.09 | 105 ± 3.6 | 14.97 | 16.11 ± 0.3 |

[a]Mean ± SEM.
[b]Estimated minimum $T_m$.
[c]Estimated minimum $\Delta T_m$.
[d]Fraction refolded is the fraction folded value for the $V_H$ at 30°C following thermal denaturation at 96°C.
[e]%Recovery was determined as described in Supplementary Fig. S4 legend.
[f]MW measurement was performed once.
NA, not applicable.

$V_H$s were more protease resistant than huVHAm302S and huVHPC235S. Previous studies showed that $V_H$Hs became protease resistant with Cys54–Cys78 disulfide linkage mutations, and that there was a positive correlation between protease resistance of $V_H$Hs and their $T_m$s (Hussack *et al.*, 2011).

### *Mutant $V_H$s are less aggregation prone than the wild-type counterparts*

Next, we investigated if the mutant $V_H$s with improved thermostability were also less aggregation prone. The effect of Cys54–Cys78 disulfide linkage mutation on protein aggregation has not been explored in the case of camelid $V_H$Hs, presumably because aggregation is not an issue with $V_H$Hs. We assessed the aggregation behavior of $V_H$s by Superdex$^{TM}$ 75 size exclusion chromatography. Typically, aggregating $V_H$s form significant amounts of multimeric/aggregating species which are distinguishable from monomeric species by their lower elution volumes on Superdex$^{TM}$ 75 size exclusion chromatograms and/or have a tendency to 'stick' to the chromatography system surfaces, e.g. column materials, resulting in lower elution recoveries and/or monomeric profiles characterized by 'tailing'. Non-aggregating $V_H$s, on the other hand, display single, symmetrical monomeric peak profiles. We found that the engineered disulfide linkage reduced $V_H$ aggregation (Fig. 2c; Table II). The wild-type $V_H$s huVHAm302 and huVHAm431 aggregated at 13.9% ± 0.02% and 5.5% ± 0.08%, respectively, which was reduced to 4.1% ± 0.15% and 4.3% ± 0.14% for the mutants (unpaired *t*-test, two-tailed, $P = 0.0002$ [huVHAm302/huVHAm302S pair]; $P = 0.0181$ [huVHAm431/huVHAm431S pair]). In the instance of huVHAm427/huVHAm427S pair, although the mutant did not show significant improvement in non-aggregation over the corresponding wild type (6.6% ± 0.76% vs. 3.8% ± 2.9%; unpaired *t*-test, two-tailed, $P = 0.4470$), the severe tailing seen in the case of the wild-type $V_H$ was rectified by the introduction of the disulfide linkage in the mutant which displayed a symmetrical monomeric peak (Fig. 2c). Clearly, this tailing cannot be due to the presence of other proteins in the $V_H$ preparation as it can be inferred from the SDS-PAGE profile of huVHAm427 (Supplementary Fig. S1). Moreover, %recovery (of monomeric species) significantly increased from 69% ± 0.6% (huVHAm302) and 82% ± 0.5% (huVHAm431) to 76% ± 0.1% and 100% ± 1.9% for mutant versions, respectively, indicating the mutants had significantly reduced stickiness (unpaired *t*-test, two-tailed, $P = 0.0070$ [huVHAm302/huVHAm302S pair] and $P = 0.0107$ [huVHAm431/huVHAm431S pair]) (Supplementary Fig. S4; Table II). Even in the case of huVHPC235, which displayed a purely monomeric profile (Fig. 2c), the introduction of the non-canonical disulfide linkage increased %recovery from 70% ± 3.7% (wild type) to 105% ± 3.6% (mutant) (unpaired *t*-test, two-tailed, $P = 0.0212$).

We confirmed by SPR and multiangle light scattering analyses that the monomeric peaks were indeed so despite their wide elution volume ($V_e$) variations (Fig. 2c: $V_e = 12.2$–15.3 ml). The SPR analysis was based on the affinity of the His tag for $Ni^{2+}$ and the observation that, because of avidity effects, proteins with more than one His tag have much slower $k_{off}$s than those with one His tag (Nieba *et al.*, 1997; Khan *et al.*, 2006). Thus, a monomeric $His_6$-tagged $V_H$ (with one $His_6$ tag) is expected to have a faster $k_{off}$ from a $Ni^{2+}$ surface than a multimeric $His_6$-tagged $V_H$ (with multiple $His_6$ tags). In SPR control experiments, a purely monomeric llama $V_H$H with one C-terminal $His_6$ tag gave $k_{off}$s of $2.71 \pm 0.01 \times 10^{-3}$ and $2.18 \pm 0.01 \times 10^{-3}$ at early and later windows of the dissociation phase when passed over a $Ni^{2+}$-immobilized sensorchip, while a purely dimeric $V_H$ with two C-terminal $His_6$ tags (Baral *et al.*, 2012) gave $k_{off}$s of $6.83 \pm 1.04 \times 10^{-5}$ and $4.21 \pm 3.92 \times 10^{-6}$ for the same dissociation phase windows, reflecting a 250- to 2000-fold slower $k_{off}$ (Fig. 2d). All the C-terminally $His_6$-tagged $V_H$s corresponding to monomeric peaks on size exclusion chromatograms gave $k_{off}$s very similar to that of the monomeric $V_H$H control, confirming their monomeric state (Fig. 2d). The SPR results were further confirmed by multiangle light scattering experiments, where it was shown that the calculated molecular weights associated with monomeric peaks ($MW_{exp}$s) were very close to their corresponding expected, formula molecular weights ($MW_{for}$s) (Table II). The molecular weights of the monomer and dimer controls were also confirmed by multiangle light scattering experiments (16.50 ± 0.35 kDa vs. 15.73 kDa [$MW_{for}$] for the monomer; 35.83 ± 1.12 kDa vs. 31.05 kDa [$MW_{for}$] for the dimer).

Reversibility of thermal unfolding, measured in terms of fraction refolded values (Fig. 2a; Supplementary Fig. S3; Table II), was not compromised by the introduction of the engineered disulfide linkage for three of four $V_H$s (unpaired *t*-test, two-tailed; $P = 0.4333$ for huVHAm302 vs. huVHA m302S; $P = 0.5412$ for huVHAm427 vs. huVHAm427S; $P = 0.2169$ for huVHPC235 vs. huVHPC235S), and in the case of huVHAm431S, was significantly improved from 0.45 (huVHAm431) to 0.89 (huVHAm431S) ($P = 0.0268$), indicating huVHAm431S acquired reduced tendency to aggregate (Barthelemy *et al.*, 2008). Thermal unfolding of mutant $V_H$s though not completely but to a large extent was reversible (fraction refolded = 0.46–0.89). However, it should be noted that fraction refolded values may be an overestimation as they may have contributions from non-active misfolded $V_H$s. Voltage values obtained on $V_H$ samples during CD measurements and visual inspection of the samples following CD measurements indicated the absence of any insoluble aggregates (Supplementary Fig. S5) (Benjwal *et al.*, 2006). The incomplete reversibility of thermal unfolding may therefore have to do, at least in part, with the formation of soluble aggregates. We also investigated the tendency of $V_H$s to form insoluble aggregates by turbidity analysis (Dudgeon *et al.*, 2012). Turbidity measurements showed that similar to a non-aggregating $V_H$H control (A4.2), all heat-treated (80°C, 20 min) wild type and mutants $V_H$s completely resisted (insoluble) aggregation. However, the formation of soluble aggregates and/or misfolded species cannot be excluded as suggested by the size exclusion chromatography and thermal unfolding data.

### *Mutant $V_H$s have altered conformations compared with the wild-type counterparts*

Previously, it was shown that the binding affinity and specificity of $V_H$Hs were altered with Cys54–Cys78 disulfide linkage mutations, suggesting that the engineered disulfide linkage altered the $V_H$H conformational structures (Chan *et al.*, 2008; Saerens *et al.*, 2008; Hussack *et al.*, 2011). To verify if the same is true for $V_H$s, we used protein A to probe $V_H$ conformation (Starovasnik *et al.*, 1999; Graille *et al.*, 2000) by determining the protein A equilibrium dissociation constants ($K_D$s) for wild type and mutant $V_H$s. We

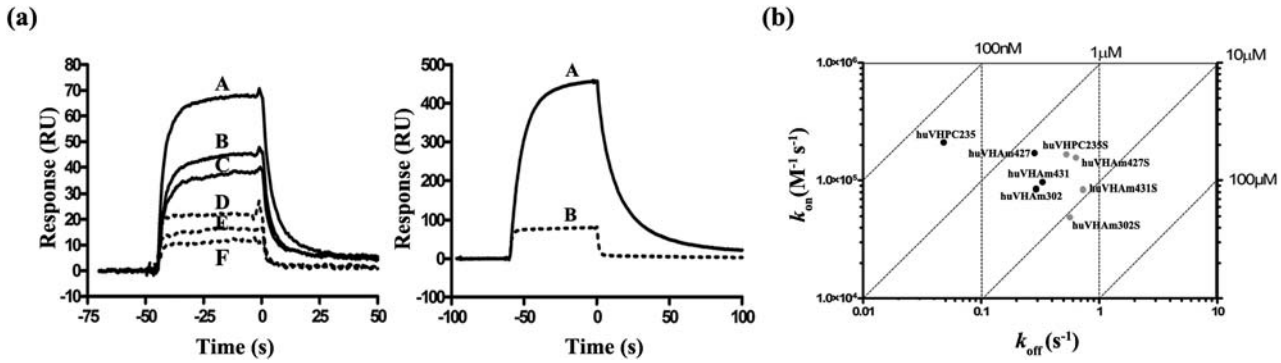


**Fig. 3.** SPR analyses of $V_H$ binding to protein A. (**a**) Biacore sensorgrams showing the binding of $V_H$s at 200 nM concentrations to immobilized protein A (see Supplementary Fig. S6 for the full range of the sensorgrams and experimental details). Wild type and mutant $V_H$ sensorgrams are shown by solid and dotted lines, respectively. On the left: A, huVHAm427; B, huVHAm302; C, huVHAm431; D, huVHAm427S; E, huVHAm431S; and F, huVHAm302S. On the right: A, huVHPC235; and B, huVHPC235S. In all cases, more binding (higher RU) is observed with wild-type $V_H$s than with mutant $V_H$s. (**b**) Rate plane with iso-affinity diagonals plot comparing wild type and mutant $V_H$s. $k_{on}$s (association rate constants), $k_{off}$s and $K_D$s were determined from SPR analyses (see Supplementary Fig. S6; Table II). Diagonal lines represent the same $K_D$.

found by SPR experiments that, compared with wild-type $V_H$s, mutant $V_H$s bound to protein A with lower affinity, indicating that the engineered disulfide linkage altered $V_H$ conformation (Fig. 3; Supplementary Fig. S6; Table II). The affinity reductions ranged from 2-fold for the huVHAm431/huVHAm431S pair to 10-fold for the huVHPC235/huVHPC235S pair. As reported previously for $V_H$Hs, the $K_D$ increases were largely and consistently due to increases in the $k_{off}$ (Fig. 3b) (Hussack *et al.*, 2011).

## Discussion

In conclusion, we have shown that the introduction of a pair of Cys residues in the core of human $V_H$ domains at positions 54 and 78 leads to the formation of Cys54–Cys78 disulfide linkage. In three $V_H$s (huVHAm302S, huVHAm427S and huVHAm431S), the formation of the Cys54–Cys78 disulfide linkage is not interfered with by the presence of CDR1 and CDR3 cysteines with disulfide linkage forming capacity, indicating that similar to the conserved Cys23–Cys104 disulfide linkage, the formation of the disulfide linkage between Cys54 and Cys78 is highly favorable (Table I). We have also shown that the introduction of the Cys54–Cys78 disulfide linkage significantly increases the thermostability of $V_H$s, as shown by $T_m$ increases of at least 14°C, without adversely affecting expression yields. Similar thermostability gains were also seen in the case of several mutant $V_H$Hs with the same non-canonical disulfide linkage (Hagihara *et al.*, 2007; Chan *et al.*, 2008; Saerens *et al.*, 2008; Hussack *et al.*, 2011). In a more recent publication, it was shown that the presence of Cys54–Cys78 disulfide linkage additionally improved the protease resistance of $V_H$Hs (Hussack *et al.*, 2011). Thus, it is very likely that the same beneficial effect exists in the case of $V_H$ domains. From the point of view of engineering for stability, the present approach appears to be generally applicable not only to $V_H$s and $V_H$Hs, but also to $V_L$s, as the introduction of Cys pairs at equivalent positions in $V_L$s also led to the formation of the intended disulfide linkage and significant increases in thermostability and protease resistance (manuscript in preparation).

We found that the engineered disulfide linkage reduced aggregation of $V_H$ domains, a significant finding considering that $V_H$ domains have the general drawback of being aggregation prone. It is likely that the improved non-aggregation of $V_H$ mutants compared with wild-type $V_H$s is due to their increased thermodynamic stability and/or having aggregation resistant unfolded states (Hussack *et al.*, 2011). However, the $V_H$ domains in this study were based on the same $V_H$ framework regions and shared a very high percentage of sequence identity. Thus, it remains to be seen if the beneficial effect of the engineered disulfide linkage in terms of improving non-aggregation is general across $V_H$ domains with differing framework regions. Barthelemy *et al.* (2008) identified non-aggregating $V_H$ domains whose non-aggregation was independent of CDR3 sequence and derived from mutations in the $V_L$ interface. However, it is very unlikely that solubilizing framework region mutations alone, including those presented in this study, can accommodate the diversity of CDR sequences (or even just CDR3 sequences) encountered in $V_H$ libraries. In other words, non-aggregation (of $V_H$s) is a function of both framework region sequence and CDR sequence (Martin *et al.*, 1997; Ewert *et al.*, 2003; Christ *et al.*, 2007), and it is very likely that synthetic $V_H$ libraries would always be populated to various degrees with aggregating $V_H$s. Thus, coupling selection for affinity to selection for non-aggregation during the panning stage of library selections (Jespers *et al.*, 2004; Famm *et al.*, 2008) is advisable even when dealing with $V_H$ libraries enriched for non-aggregating domains (Christ *et al.*, 2007), as the approach increases the likelihood of obtaining non-aggregating $V_H$ binders.

Using protein A as a structural sensor, we found that the introduction of the Cys54–Cys78 disulfide linkage led to conformational changes in the backbone of mutant $V_H$s. This is conceivable as the engineered disulfide linkage connects, and possibly alters, the β-strands (C′ and D) which are presumably involved in protein A binding (Riechmann and Davies, 1995; Starovasnik *et al.*, 1999). The differential effect of the engineered disulfide linkage on $V_H$ affinity, as also seen previously with $V_H$Hs (Hussack *et al.*, 2011), suggests that the Cys54–Cys78 disulfide linkage alters the structure of $V_H$s to a different extent. We cannot comment with certainty on the effect of the engineered disulfide linkage on antigen affinity of $V_H$s since we were not able to obtain affinity values for wild-type $V_H$s: in the case of huVHPC235 the antigen was not known, and in the case of amylase

binders huVHAm302, huVHAm427 and huVHAm431 (Arbabi-Ghahroudi *et al.,* 2009b), the tendency of $V_H$s to aggregate precluded reliable affinity measurements by SPR. However, it is likely that the conformational changes observed through protein A measurements would transmit through paratopes leading to affinity and specificity compromises in $V_H$ binders as has been demonstrated with $V_H$Hs (Chan *et al.*, 2008; Saerens *et al.*, 2008; Hussack *et al.*, 2011). Thus, to avoid this drawback, one may start the selection for binders from synthetic $V_H$ libraries—which are, after all, the source of $V_H$ binders—that already have the Cys54–Cys78 disulfide linkage feature. Such $V_H$ libraries which would be generated by CDR randomization on stable scaffolds with the Cys54–Cys78 disulfide linkage mutation should also be a richer source of binders with characteristics such as high expression, thermostability, protease resistance and non-aggregation compared with the same libraries built on the wild-type scaffolds. Furthermore, the efficiency of isolating binders with such desirable characteristics would increase, should the selection be performed under stability pressure as has been successfully demonstrated (Jespers *et al.*, 2004; Famm *et al.*, 2008; Arbabi-Ghahroudi *et al.*, 2009b).

We demonstrated that an SPR-based assay based on the $Ni^{2+}$–$His_6$ tag interaction, and involving flowing His-tagged $V_H$s over $Ni^{2+}$-immobilized sensorchip surfaces, can be employed to distinguish between monomeric and multimeric $V_H$s. The approach can be used as a complement or alternative to size exclusion chromatography for assessing the aggregation status of $V_H$s or other antibody fragments. As the minimal requirements for the assay were a few pmol of protein at a concentration as low as 50 nM, it should be applicable to high-throughput screening of non-aggregating $V_H$s (or other His-tagged proteins) expressed on a small scale. Moreover, the screening may be applied directly to unpurified $V_H$ samples in cell extracts since the His-tagged protein purification should occur as the cell extracts flow over the $Ni^{2+}$ sensorchip surfaces.

Taken together, our study presents a novel approach for efficacy engineering of $V_H$-based biologics. Given the structural similarities between $V_H$s and $V_L$s, the approach should be applicable to $V_L$-based biologics as well. Furthermore, libraries based on the $V_H$ scaffold with the Cys54–Cys78 disulfide linkage feature—in particular those based on the highly thermodynamically stable human $V_H$3 family sequences (Ewert *et al.,* 2003)—should provide a wider depth and breadth in terms of affinity and specificity range compared with the same libraries based on the wild-type $V_H$ scaffold due to the higher stability and the reduced loss of library members to aggregation.

## Supplementary data

Supplementary data are available at *PEDS* online.

## Acknowledgements

The authors thank Sonia Leclerc for DNA sequencing and Aaron Cowan for careful reading of the manuscript.

## References

Amzel,L.M. and Poljak,R.J. (1979) *Annu. Rev. Biochem.*, **48**, 961–997.
Arbabi-Ghahroudi,M., MacKenzie,R. and Tanha,J. (2009a) *Methods Mol. Biol.*, **525**, 187–216, xiii.
Arbabi-Ghahroudi,M., To,R., Gaudette,N., Hirama,T., Ding,W., MacKenzie,R. and Tanha,J. (2009b) *Protein Eng. Des. Sel.*, **22**, 59–66.
Arbabi-Ghahroudi,M., MacKenzie,R. and Tanha,J. (2010) *Methods Mol. Biol.*, **634**, 309–330.
Baral,T.N., Chao,S.-Y., Li,S., Tanha,J., Arbabi-Ghahroudi,M., Zhang,J. and Wang,S. (2012) *PLoS ONE*, **7**, e30149.
Barthelemy,P.A., Raab,H., Appleton,B.A., Bond,C.J., Wu,P., Wiesmann,C. and Sidhu,S.S. (2008) *J. Biol. Chem.*, **283**, 3639–3654.
Benjwal,S., Verma,S., Röhm,K.-H. and Gursky,O. (2006) *Protein Sci.*, **15**, 635–639.
Betz,S.F. (1993) *Protein Sci.*, **2**, 1551–1558.
Chan,P.H., Pardon,E., Menzer,L., *et al.* (2008) *Biochemistry*, **47**, 11041–11054.
Choi,S., Jeong,J., Na,S., Lee,H.S., Kim,H.Y., Lee,K. and Paek,E. (2010) *J. Proteome Res.*, **9**, 626–635.
Christ,D., Famm,K. and Winter,G. (2007) *Protein Eng. Des. Sel.*, **20**, 413–416.
Ciaccio,N.A. and Laurence,J.S. (2009) *Mol. Pharm.*, **6**, 1205–1215.
Davies,J. and Riechmann,L. (1996) *Protein Eng.*, **9**, 531–537.
Dombkowski,A.A. (2003) *Bioinformatics*, **19**, 1852–1853.
Dudgeon,K., Rouet,R., Kokmeijer,I., Schofield,P., Stolp,J., Langley,D., Stock,D. and Christ,D. (2012) *Proc. Natl. Acad. Sci. U. S. A.*, **109**, 10879–10884.
Ewert,S., Huber,T., Honegger,A. and Plückthun,A. (2003) *J. Mol. Biol.*, **325**, 531–553.
Famm,K., Hansen,L., Christ,D. and Winter,G. (2008) *J. Mol. Biol.*, **376**, 926–931.
Fersht,A.R. (1997) *Curr. Opin. Struct. Biol.*, **7**, 3–9.
Frokjaer,S. and Otzen,D.E. (2005) *Nat. Rev. Drug Discov.*, **4**, 298–306.
Gong,R., Vu,B.K., Feng,Y., Prieto,D.A., *et al.* (2009) *J. Biol. Chem.*, **284**, 14203–14210.
Goto,Y. and Hamaguchi,K. (1979) *J. Biochem.*, **86**, 1433–1441.
Govaert,J., Pellis,M., Deschacht,N., Vincke,C., Conrath,K., Muyldermans,S. and Saerens,D. (2012) *J. Biol. Chem.*, **287**, **1970–1979**.
Graille,M., Stura,E.A., Corper,A.L., Sutton,B.J., Taussig,M.J., Charbonnier,J.B. and Silverman,G.J. (2000) *Proc. Natl. Acad. Sci. U. S. A.*, **97**, 5399–5404.
Hagihara,Y., Mine,S. and Uegaki,K. (2007) *J. Biol. Chem.*, **282**, 36489–36495.
Ho,S.N., Hunt,H.D., Horton,R.M., Pullen,J.K. and Pease,L.R. (1989) *Gene*, **77**, 51–59.
Horwich,A. (2002) *J. Clin. Invest.*, **110**, 1221–1232.
Hurle,M.R., Helms,L.R., Li,L., Chan,W. and Wetzel,R. (1994) *Proc. Natl. Acad. Sci. U. S. A.*, **91**, 5446–5450.
Hussack,G., Hirama,T., Ding,W., MacKenzie,R. and Tanha,J. (2011) *PLoS ONE*, **6**, e28218.
Jespers,L., Schon,O., Famm,K. and Winter,G. (2004) *Nat. Biotechnol.*, **22**, 1161–1165.
Khan,F., He,M. and Taussig,M.J. (2006) *Anal. Chem.*, **78**, 3072–3079.
Kim,D.Y., Ding,W. and Tanha,J. (2012) *Methods Mol. Biol.*, **911**, 355–372.
Mansfeld,J., Vriend,G., Dijkstra,B.W., Veltman,O.R., van den Burg,B., Venema,G., Ulbrich-Hofmann,R. and Eijsink,V.G.H. (1997) *J. Biol. Chem.*, **272**, 11152–11156.
Martin,F., Volpari,C., Steinkuhler,C., *et al.* (1997) *Protein Eng.*, **10**, 607–614.
Mason,J.M., Gibbs,N., Sessions,R.B. and Clarke,A.R. (2002) *Biochemistry*, **41**, 12093–12099.
Matsumura,M., Signor,G. and Matthews,B.W. (1989) *Nature*, **342**, 291–293.
Mitraki,A. and King,J. (1992) *FEBS Lett.*, **307**, 20–25.
Nieba,L., Nieba-Axmann,S.E., Persson,A., *et al.* (1997) *Anal. Biochem.*, **252**, 217–228.
Proba,K., Wörn,A., Honegger,A. and Plückthun,A. (1998) *J. Mol. Biol.*, **275**, 245–253.
Riechmann,L. and Davies,J. (1995) *J. Biomol. NMR*, **6**, 141–152.
Saerens,D., Conrath,K., Govaert,J. and Muyldermans,S. (2008) *J. Mol. Biol.*, **377**, 478–488.
Starovasnik,M.A., O'Connell,M.P., Fairbrother,W.J. and Kelley,R.F. (1999) *Protein Sci.*, **8**, 1423–1431.
To,R., Hirama,T., Arbabi-Ghahroudi,M., MacKenzie,R., Wang,P., Xu,P., Ni,F. and Tanha,J. (2005) *J. Biol. Chem.*, **280**, 41395–41403.
Ward,E.S., Güssow,D., Griffiths,A.D., Jones,P.T. and Winter,G. (1989) *Nature*, **341**, 544–546.
Wetzel,R. (1994) *Trends Biotechnol.*, **12**, 193–198.
Wetzel,R., Perry,L.J., Baase,W.A. and Becktel,W.J. (1988) *Proc. Natl. Acad. Sci. U. S. A.*, **85**, 401–405.
Williams,A.F. and Barclay,A.N. (1988) *Annu. Rev. Immunol.*, **6**, 381–405.

Wörn,A. and Plückthun,A. (2001) *J. Mol. Biol.*, **305**, 989–1010.
Wozniak-Knopp,G., Stadlmann,J. and Rüker,F. (2012) *PLoS ONE*, **7**, e30083.
Wu,S.L., Jiang,H., Lu,Q., Dai,S., Hancock,W.S. and Karger,B.L. (2009) *Anal. Chem.*, **81**, 112–122.
Young,N.M., MacKenzie,C.R., Narang,S.A., Oomen,R.P. and Baenziger,J.E. (1995) *FEBS Lett.*, **377**, 135–139.